

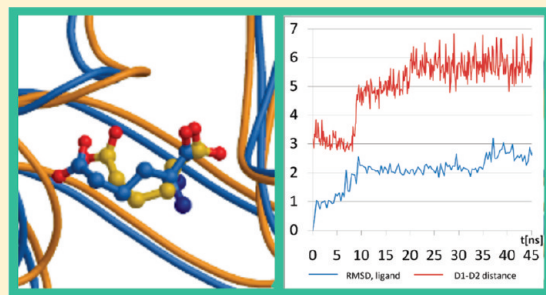
Full and Partial Agonism of Ionotropic Glutamate Receptors Indicated by Molecular Dynamics Simulations

Pekka A. Postila, Mikko Ylilauri, and Olli T. Pentikäinen*

Department of Biological and Environmental Science, P.O. Box 35, University of Jyväskylä, FI-40014, Finland

 Supporting Information

ABSTRACT: Ionotropic glutamate receptors (iGluRs) are synaptic proteins that facilitate signal transmission in the central nervous system. Extracellular iGluR cleft closure is linked to receptor activation; however, the mechanism underlying partial agonism is not entirely understood. Full agonists close the bilobed ligand-binding domain (LBD), while antagonists prevent closure; the transmembrane ion channel either opens or stays closed, respectively. Although some bulky partial agonists produce intermediate iGluR-LBD closure, the available crystal structures also imply that the cleft can be shut with certain partial agonists. Recently, we have shown that the iGluR-LBD closure stage can be recreated by inserting a ligand into the closed cleft and simulating the ligand–receptor complex with molecular dynamics. Our simulations indicate that partial agonist binding does not necessarily prevent full receptor cleft closure; instead, it destabilizes cleft closure. Interdomain hydrogen bonds were studied thoroughly, and one hydrogen bond, in particular, was consistently disrupted by bound partial agonists. Accordingly, the simulation protocol presented here can be used to categorize compounds *in silico* as partial or full agonists for iGluRs.



INTRODUCTION

Ionotropic glutamate receptors (iGluRs) mediate neuronal stimuli in the synapses of the central nervous system. The iGluR monomer is composed of the extracellular N-terminal domain and the ligand-binding domain (LBD), four transmembrane regions, and the cytoplasmic C-terminus. The binding of a full agonist to the receptor cleft between the D1 and D2 lobes closes the LBD¹ (Figure 1). The closure of the iGluR-LBD, in turn, rearranges the transmembrane regions, which form the ion channel in the iGluR tetramer complex,^{2,3} and an influx of cations depolarizes the postsynaptic neuron. The iGluR family is divided into kainate, N-methyl-D-aspartate (NMDA), and 2-amino-3-(3-hydroxy-5-methyl-4-isoxazolyl)propionic acid (AMPA) receptors, according to their ligand-binding specificities and sequence differences.⁴ L-glutamate (Figure 2) is the natural neurotransmitter (or full agonist) for all iGluR subunits except GluN1 (GLU_{N1}; NMDA-R1), which binds a smaller amino acid, glycine (Figure 2).⁵ Antagonists block the closure of iGluR-LBD or its counterpart ligand-binding core (LBC; Figure 1), which is isolated for crystallization, and prevent agonist binding;^{6–9} thus, the receptor stays inactive. Partial agonists produce partial activation or weaker maximum responses than the endogenous neurotransmitter L-glutamate, which has also been shown to cause intermediate or partial iGluR cleft closure^{6,10–13} (Figure 1).

We have previously reproduced the intermediate closure of GluK1-LBC (GLU_{K5}; GluRS) with the partial agonists kainate and domoate (Figure 2) and predicted the closure with dysihabaine analog 9-deoxy-neoDH using all-atom molecular dynamics (MD) simulations with an explicit solvent.¹⁴ However, it is

possible that intermediate iGluR cleft closure is not always required for partial agonism. MSVIII-19 (or 8,9-deoxy-neoDH), which is a very weak partial agonist or a functional antagonist for kainate receptors,¹⁵ preferred the closed GluK1 cleft in both our MD simulations^{14,16} and our crystallographic study.¹⁷ The MSVIII-19-GluK1 simulations suggested that interdomain cleft closure stability could be an indicator of desensitization,¹⁴ and with MSVIII-19 and 5-substituted derivatives of willardiine (or 5-R-willardiines; Figure 2), the swiftness of desensitization is known to influence receptor activation.^{15,18} Moreover, 5-R-willardiines keep the GluA2 (GLU_{A2}; GluR2) cleft only moderately open and, yet, act as partial agonists.¹¹ There is also a set of small partial agonists for GluK2 (GLU_{K6}; GluR6; Figure 2), which, according to a docking study by Fay et al., prefers closed conformation.¹⁹ The dimer interface rearrangement that occurs after the ion channel opens,²⁰ as well as modulation by anions, also contributes to iGluR desensitization.²¹ In addition, the antagonist 6,7-dinitroquinoxaline-2,3-dione (DNQX), which keeps the GluA2 cleft fully open, is, in fact, a weak partial agonist, if coexpressed with transmembrane AMPA receptor regulatory proteins.²²

In this study, we wanted to determine whether partial agonists could reliably be distinguished from full agonists by inspecting the D1–D2 interactions of iGluR-LBCs in MD simulations. To acquire a complete picture of partial agonism, we simulated a large set of partial and full agonists that are specific to GluA2,

Received: January 6, 2011

Published: April 18, 2011

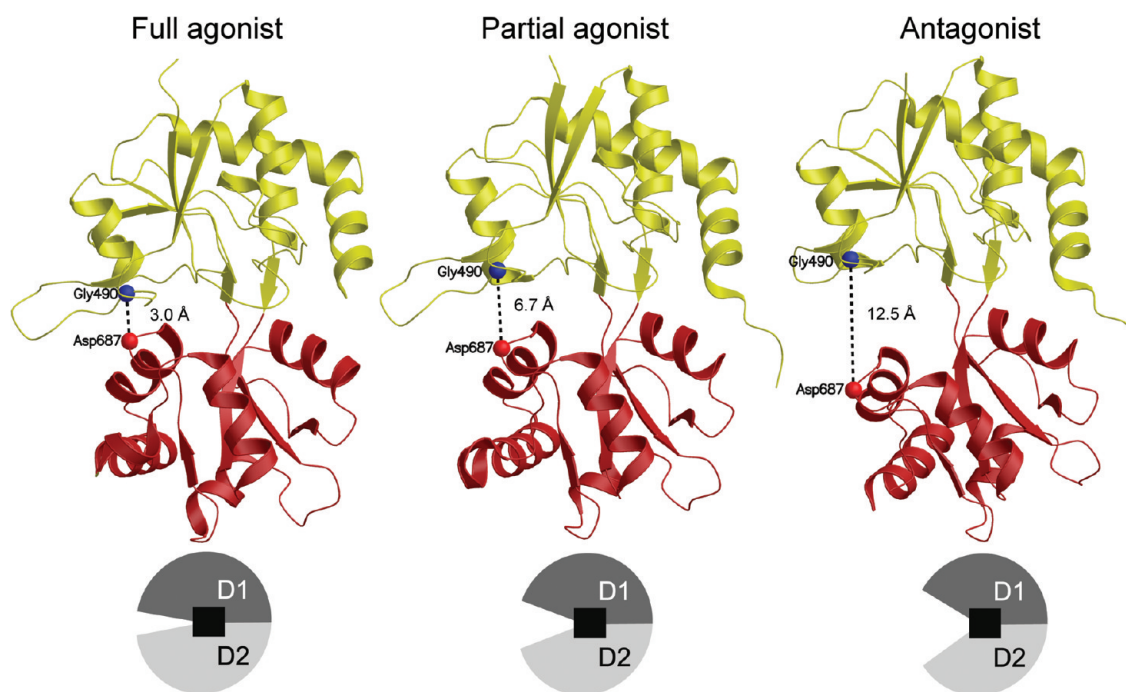


Figure 1. The hydrogen-bonding (H-bonding) distance indicates full and partial agonism and antagonism in iGluR crystal structures. (A) Full agonist L-glutamate causes full GluK1-LBC closure (PDB: 1YCJ) that is also indicated by an interdomain hydrogen bond (IHB) between Gly490^N and Asp687^O (3.0 Å). (B) Partial agonist domoate induces intermediate GluK1 cleft closure (PDB: 2PBW) indicated by the nonbonding distance between IHB atom pair Gly490^N and Asp687^O (6.7 Å). (C) Antagonist (S)-ATPO keeps the GluK1 cleft fully open (PDB: 1VSO) also without Gly490^N-Asp687^O H-bonding (12.5 Å). The dotted lines indicate the distances between the IHB atom pair in GluK1-LBC crystal structures; however, the H-bond is only formed in full agonist-GluK1 complex (3.0 Å). For clarity the bound ligands in the ligand-binding site (black box) are not shown. The D1 lobe is colored with yellow and the D2 lobe with red.

GluK2, and GluN1 receptors (Figure 2). Our results indicate that some partial agonists are not able to partially open the iGluR cleft when it is in the closed conformation. Instead, these partial agonists frequently break a particular hydrogen bond (H-bond) situated in the receptor clefts of GluA2 and GluN1 subunits. The results indicate that this H-bond also plays a critical role in the partial agonism of GluK2; on the other hand, differences in the stability of the GluK2 cleft closure between full and partial agonists are less pronounced. Thus, our results demonstrate that the disruption of interdomain H-bonding is enough to distinguish at least GluA2 and GluN1 specific partial agonists from full agonists.

MATERIALS AND METHODS

Protein Structures. The crystal structures used in MD simulations of iGluR-LBCs were acquired from the PDB.²³ The MD simulations of GluK2-LBC monomer with L-glutamate (PDB: 1SS0, A chain),¹² kainate (PDB: 1TT1, A chain),¹² domoate (PDB: 1YAE, B chain),¹³ and SYM 2081 (PDB: 1SD3, A chain)¹² were run using their original crystal structures. Likewise original crystal structures were used in GluA2-LBC monomer MD simulations with L-glutamate (PDB: 1FTJ, C chain),⁶ AMPA (PDB: 1FTM, A chain),⁶ willardiine (PDB: 1MQJ, A chain),¹¹ S-Br-willardiine (PDB: 1MQH, A chain),¹¹ S-F-willardiine (PDB: 1MQI, A chain),¹¹ S-I-willardiine (PDB: 1MQG, A chain),¹¹ and without a ligand (PDB: 1FTO, A chain).⁶ For the 5-Cl-willardiine-GluA2 simulation, the 5-Br-willardiine-GluA2 crystal structure¹¹ was used after the 5-bromo was substituted with a 5-chloro group. The complete kainate-GluA2

complex without a missing loop was built based on the alignment of the crystal structure (PDB: 1FTK, A chain)⁶ and the rat sequence (GRIA2)²⁴ using MALIGN in BODIL²⁵ and MODELLER9v7.²⁶ Similarly the complete structures of GluN1-LBC monomers with glycine (PDB: 1PB7),¹⁰ D-serine (PDB: 1PB8),¹⁰ ACPC (PDB: 1Y20),²⁷ and D-cycloserine (PDB: 1PB9)¹⁰ were built based on the alignment of the correspondent crystal structure and the rat sequence (GRIN1)²⁸ using MALIGN in BODIL and NEST.²⁹

Ligand Structures and Positioning. To acquire closed iGluR cleft conformation for all ligand-iGluR complexes, the ligand positioning was obtained from the available crystal structures by superimposing them with C^α-atoms with the closed GluK2-LBC (PDB: 1SS0, A chain) or the closed GluA2-LBC (PDB: 1FTM, A chain) using VERTAA in BODIL. The 3D ligand structures were prepared with SYBYL7.3 (Tripos, Inc., St Louis, MO) and optimized quantum mechanically with GAUSSIAN03 (Gaussian Inc., Wallingford, CT) at the HF/6-31+G* level using a polarizable continuum model (PCM). The atom-centered point charges were calculated from the electrostatic potentials with the restrained electrostatic potential (RESP) methodology.^{30–32} With 5-I-willardiine, HF/3-21G and Merz-Kollman radius of 2.3 for iodine³³ was used, because iodine is not included in HF/6-31+G* basis set. The optimized partial agonists for GluK2 (Figure 2) except domoate were docked flexibly into the closed GluK2-LBC with GOLD3.1^{34,35} using search area of a 15 Å radius sphere centered at the O^{OH/O₃}-atom of Tyr488 in the ligand-binding site. The structure comparisons demonstrate that the initial ligand conformations used in the closed iGluR-LBC simulations were stable (Figure S1, Supporting Information).

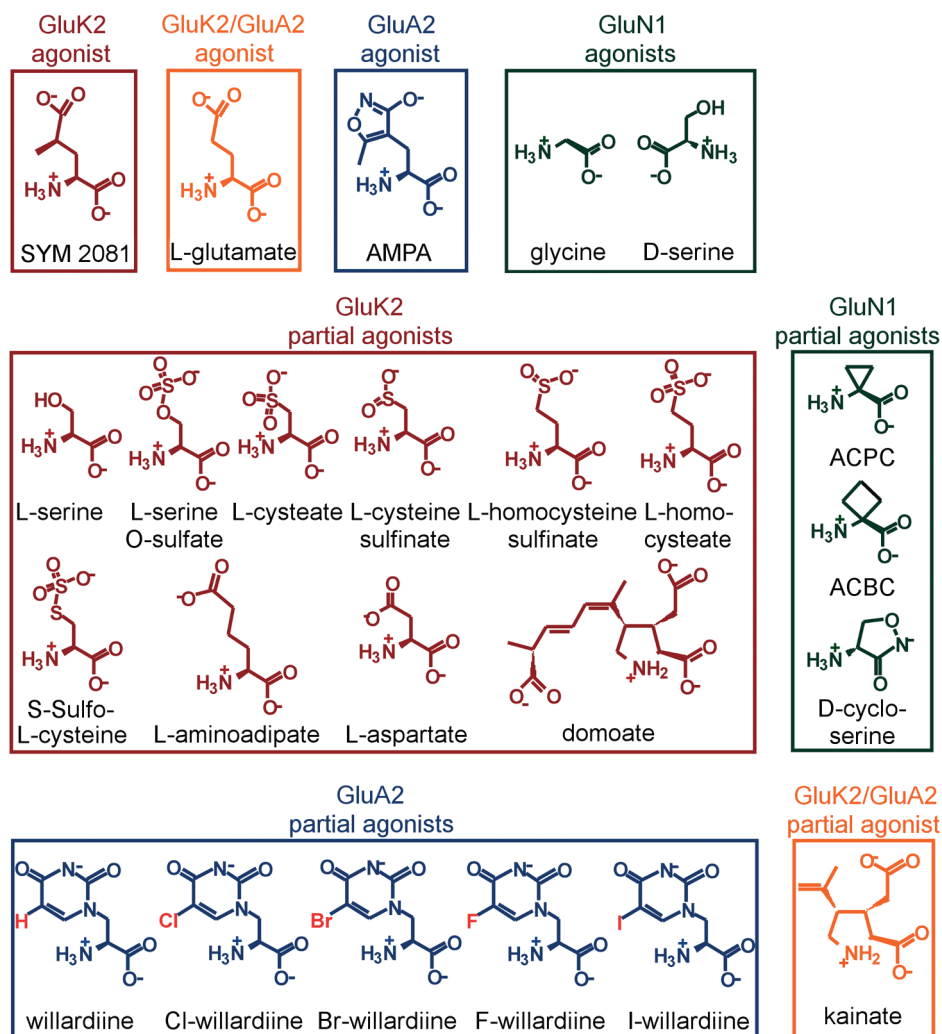


Figure 2. The two-dimensional (2D) structures of all MD simulated full and partial agonists. The ligands are boxed into receptor subunit specific groups: GluK2 (red), GluA2 (blue), GluN1 (green), and shared GluA2 and GluK2 (orange).

Ligand–Receptor Complexes for MD. The charges were set equal for chemically comparable atoms for each ligand. The protonation of histidines was selected on the basis of H-bonding with nearby residues and water molecules. Water molecules situated 1.4 Å radius of the ligand were removed using BODIL in cases where original crystal structure was not used. TLEAP in ANTECHAMBER-1.27³⁶ was used to: (1) generate the force field parameters for the protein (parm99) and ligands (gaff); (2) add hydrogen atoms; (3) neutralize the system with sodium or chloride ions; and (4) solvate the system with a rectangular box of transferable intermolecular potential three-point water molecules 13 Å in every dimension.

MD Simulations. NAMD 2.6³⁷ was used for the energy minimization and MD steps. All protein–ligand systems were equilibrated in three steps: (1) The water molecules, counterions, and amino acid side chains were energy minimized with the conjugate gradient algorithm (15 000 steps), whereas the rest of the system was constrained by restraining C^α-atoms with the harmonic force of 5 kcal mol⁻¹ Å⁻²; (2) the whole system was energy minimized without constraints (15 000 steps); and (3) a MD simulation was performed with restrained C^α-atoms in constant pressure (30 000 steps). The production simulation

was repeated three times (six times with SYM 2081) using the same setup without constraints for 46 ns with all ligand–receptor complexes to ensure reliable results. All steps were run in constant volume. The complex was held at 300 K with Langevin dynamics for all nonhydrogen atoms, using a Langevin damping coefficient of 5 ps⁻¹. Nosé-Hoover Langevin piston³⁸ kept pressure at 1 atm with an oscillation time scale of 200 fs and a damping time scale of 100 fs. An integration time step of 2 fs was used under a multiple time stepping scheme.³⁹ The bonded and short-range interactions were calculated every time step and the long-range electrostatic interactions every third step. A cutoff of 12 Å was used for the short-range electrostatic interactions and the van der Waals forces. A switching function smoothed the van der Waals forces cutoff. The simulations were run under the periodic boundary conditions, and the long-range electrostatics were counted with the particle mesh Ewald method.^{40–43} The H-bonds were restrained with the SHAKE algorithm.⁴⁴

Trajectory Analysis. Snapshot structures at 360 ps intervals were extracted from the MD trajectories with PTraj in ANTECHAMBER 1.27³⁶ to visually ensure the integrity of the simulated systems. Various atom distances and closure angles were

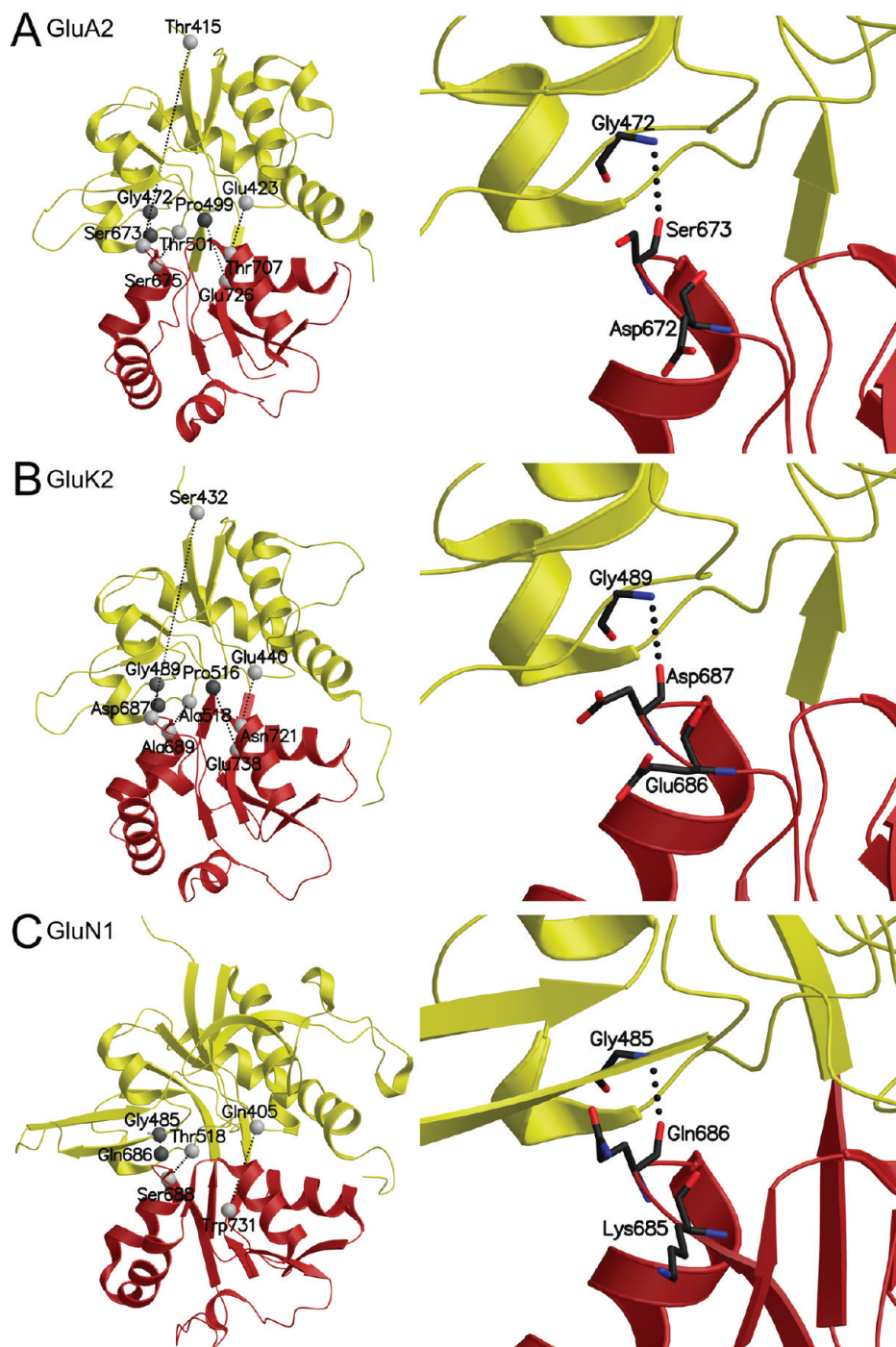


Figure 3. The interdomain distances and H-bonds measured between the D1 and D2 lobes. (A) The measured atom pairs for GluA2 include: Pro499^O-Glu726^{Cα}, Ser675^{Cα}-Thr501^{Cα}, Thr415^{Cα}-Ser673^{Cα}, and Gly472^N-Ser673^O (IHB; close-up in right panel), and the H-bonding distance between the side chains of Glu423 and Thr707 (shown with C^α-atoms). (B) The atom pairs at equivalent positions in the 3D space in GluK2-LBC are Pro516^O-Glu738^{Cα}, Ala689^{Cα}-Ala518^{Cα}, Ser432^{Cα}-Asp687^{Cα}, and Gly489^N-Asp687^O (IHB; close-up in right panel) and the H-bonding between the side chains of Glu440 and Asn721. (C) With GluN1, Thr518^{Cα}-Ser688^{Cα} and Gly485^N-Gln686^O (IHB; close-up in right panel) and H-bonding distance between the side chains of Gln405 and Trp731 were measured. The D1 lobe is colored with yellow and the D2 lobe with red.

measured with PTraj from key residues in the ligand-binding pockets (Figure 3). All distances and angles were measured at 120 ps intervals. The angles for the cleft closure were measured by using three different triangles; however, none of them describe the closure of the cleft as efficiently as simple distance measurement. The fluctuation in MD simulations is more

distracting when the cleft closure dynamics were measured using the triangles instead of simple atom pair distances (Figure S2, Supporting Information). The cutoff value of 3.4 Å was used as the upper limit for an H-bonding distance. Moreover, the movements of the D1 and D2 domains were studied thoroughly by superimposing the snapshot structures with the C^α-atoms

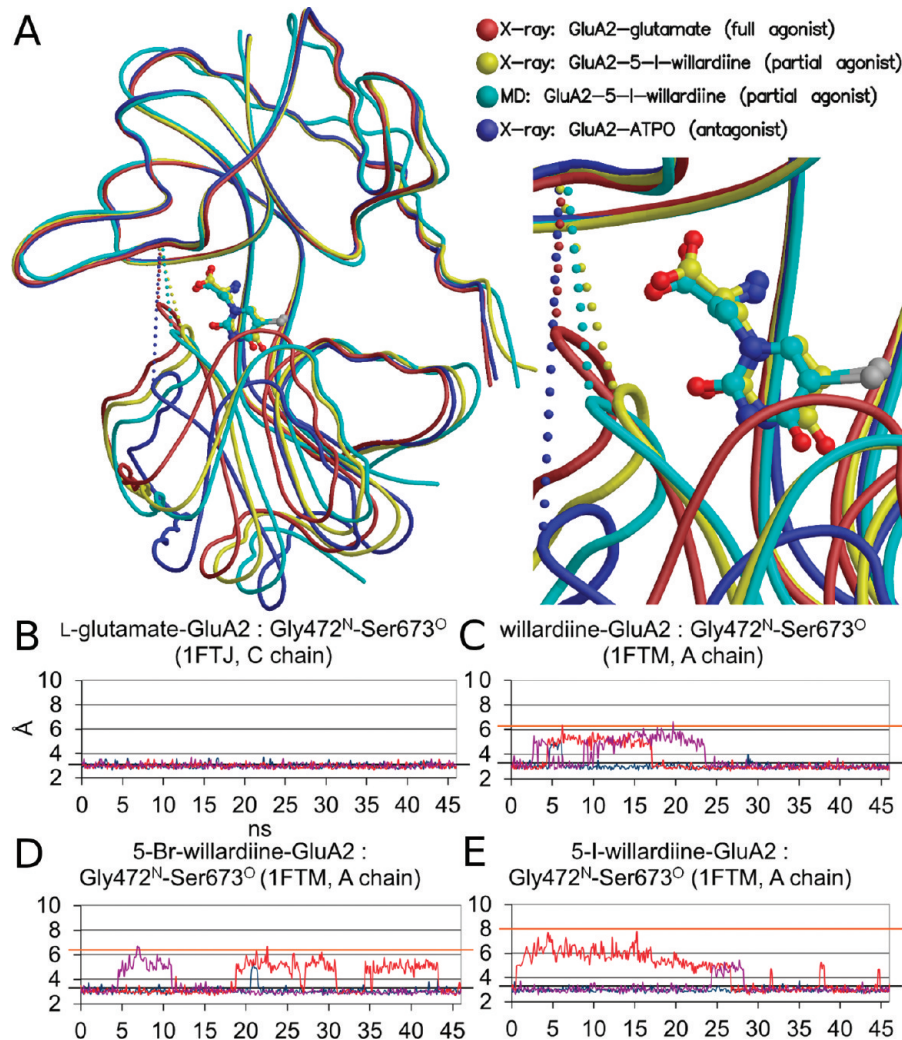


Figure 4. Full and partial agonist simulations with GluA2. (A) The structure comparison of GluA2 crystal structures with bound full agonist L-glutamate (PDB: 1FTJ, C chain; red), partial agonist 5-I-willardiine (PDB: 1MQG; yellow), and antagonist (S)-ATPO (PDB: 1N0T; blue) shows clear conformational shift. The close-up of the IHB distance (dotted lines; Figure 3A: right panels) shows that the initially closed cleft of 5-I-willardiine-GluA2 complex (PDB: 1FTM; cyan) is able to open partially during MD simulation (snapshot of ~15 ns from no. 2 simulation in panel E; red line). This simulated GluA2 cleft opening (cyan), which also breaks the IHB (Figure 3A: right panel), is at an equivalent level with the 5-I-willardiine-GluA2 crystal structure (yellow). (B) The closed GluA2-LBC (PDB: 1FTJ, C chain) stays stably closed in all three L-glutamate-bound simulations. However, the IHB of the closed GluA2-LBC opened temporarily (C) with partial agonists willardiine, (D) 5-Br-willardiine, and (E) 5-I-willardiine. The orange lines indicate the IHB distance acquired from original 5-R-willardiine-GluA2 crystal structures.¹¹ The black line indicates the IHB distance taken from the crystal structure used as a starting conformation for the simulations.⁶ The blue, red, and magenta (simulations 1–3, respectively, in Table S2, Supporting Information) lines indicate three separate MD simulations performed with the same ligand–receptor complex.

using BODIL (data not shown). In addition, the ligand positioning was inspected by extracting root-mean-square deviation (RMSD) values against the starting structure with PTTRAJ (Figure S1, Supporting Information).

Figures. Figures 1, 3, 4A, 5A, and 6A were generated using BODIL, MOLSCRIPT,⁴⁵ and RASTER3D.⁴⁶ For clarity, the coil option in MOLSCRIPT was utilized when visualizing the structure comparisons in Figures 4A, 5A, and 6A.

RESULTS AND DISCUSSION

Key Interdomain H-Bond Indicates When the Receptor Cleft Is Open or Closed. A variety of interdomain distances (Figure 3) were measured using the MD simulation trajectories, to indicate the effects of ligand binding on iGluR cleft closure.

Particular effort was put into examining interdomain H-bonding, as this has been shown to play an important role in iGluR cleft closure and receptor function.^{47–50} Although the interdomain H-bond between the side chains of Glu423 and Thr707 with GluA2 (Glu440 and Asn721 with GluK2; Gln405 and Trp731 with GluN1; Figure 3) has been reported to influence receptor cleft closure stability, recovery from desensitization,⁵⁰ and cell membrane trafficking,^{47,49} it did not differ between full agonists and partial agonists (shown for GluA2 in Table S1, Supporting Information). However, the Gly472^N-Ser673^O H-bond with GluA2 (Gly489^N-Asp687^O with GluK2; Gly485^N-Gln686^O with GluN1; Figure 3: right panels) differed consistently between full and partial agonists; accordingly, we focus here on this particular interdomain H-bond (hereafter referred to as IHB). Moreover, the IHB atom distance is an excellent indicator of full and partial

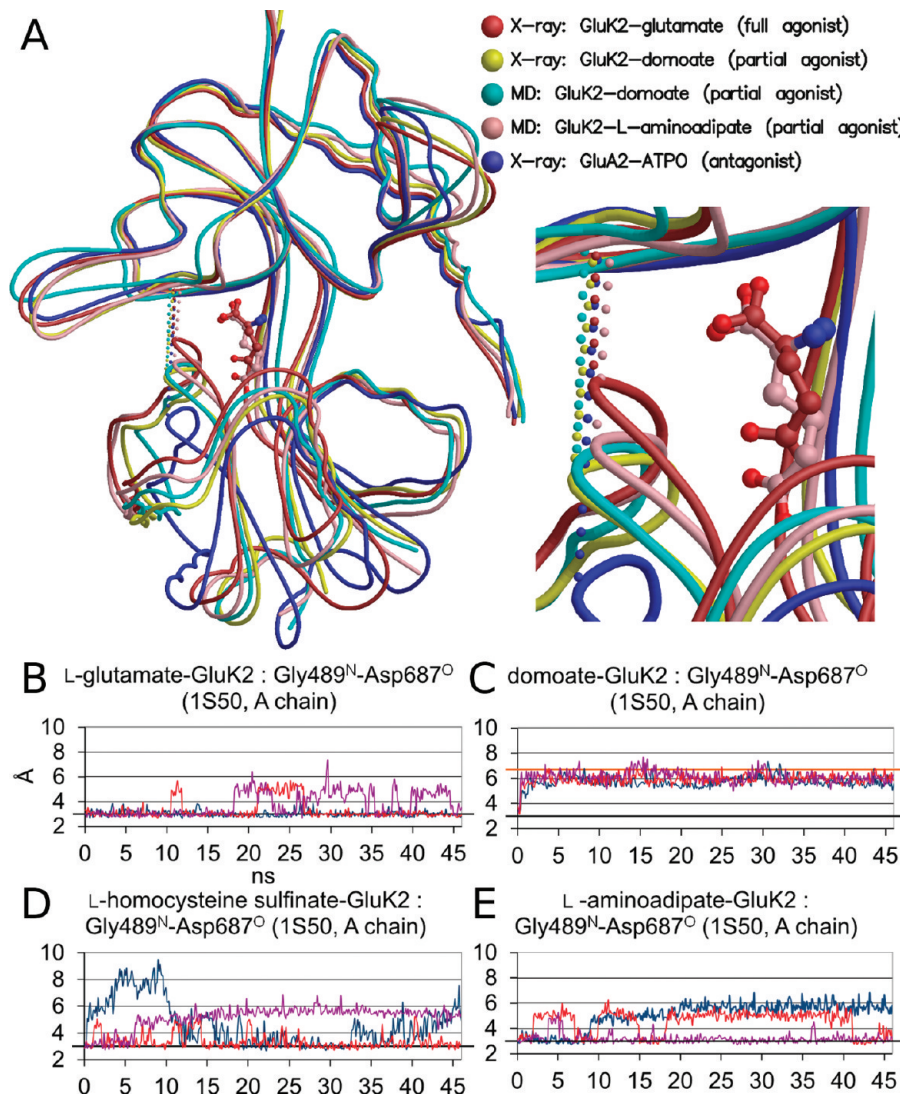


Figure 5. Full and partial agonist simulations with GluK2. (A) The structure comparison indicates clear conformational shift between the GluK2 crystal structures bound by full agonist L-glutamate (PDB: 1S50, chain A; red), partial agonist domoate (PDB: 1YAE; yellow), and GluA2 with bound antagonist (S)-ATPO (PDB: 1N0T; blue). The close-up of IHB distance (dotted lines; Figure 3A: right panel) shows that bulky partial agonist domoate (cyan) is able to open the fully closed GluK2 cleft (PDB: 1S50, chain A) during the MD simulation. The MD simulated opening (snapshot of ~15 ns from no. 1 simulation in panel C; blue line) almost reaches the level seen in domoate-GluK2 crystal structure (yellow). However, with small partial agonist L-amino adipate the GluK2 cleft opening is less pronounced, although the IHB distance widened from the initial stage (red). The IHB stays formed with (B) full agonist L-glutamate but with partial agonists (C) domoate, (D) L-homocysteine sulfinate, and (E) L-amino adipate the closed GluK2-LBC (PDB: 1S50) opens and IHB breaks in the MD simulations. The orange line indicates IHB distance acquired from domoate-GluA2 complex crystal structure.¹³ See Figure 4 for interpretation.

agonism and antagonism (or cleft closure angle, in general), as indicated, for example, by GluK1 crystal structures (Figure 1) and our previous modeling results.¹⁴

Full Agonists for GluA2 Keep the Receptor Cleft Closed.

The GluA2 cleft has been crystallized into several closure stages according to what kind of ligand is bound to it (Figure 4A). Although these crystal structures give a good overall picture on how the cleft closure is linked to receptor function, they do not provide mechanistic details on the cleft closure dynamics. Therefore, our aim was to study how the cleft closure dynamics differed between full and partial agonist-bound iGluR-LBCs using MD simulations. First we ran simulations with known full agonist GluA2 complex crystal structures (Figure 2) to determine the closed GluA2 receptor cleft dynamics. In full agonist L-glutamate-GluA2

(Figure 4B) and AMPA-GluA2 complex (Figure S3, Supporting Information) simulations, the IHB remained firmly formed (Table S2, Supporting Information) as the receptor cleft was also shut. This GluA2 cleft closure stability was also supported indirectly by the relative immobility and low RMSD value of the bound L-glutamate ($0.95 \pm 0.21 \text{ \AA}$, Figure S1, Supporting Information).

5-Substituted Willardiines Disrupt GluA2 Cleft H-Bonding. The partial cleft closure stages of 5-R-willardiine-GluA2 crystal structures (Figures 2 and 4A, Table S2, Supporting Information) follow the size of the 5-substituent,¹¹ and, accordingly, the IHB is not formed in these complexes (Table S2, Supporting Information). When the 5-R-willardiines were inserted into the closed GluA2-LBC, the IHB did not remain broken in most

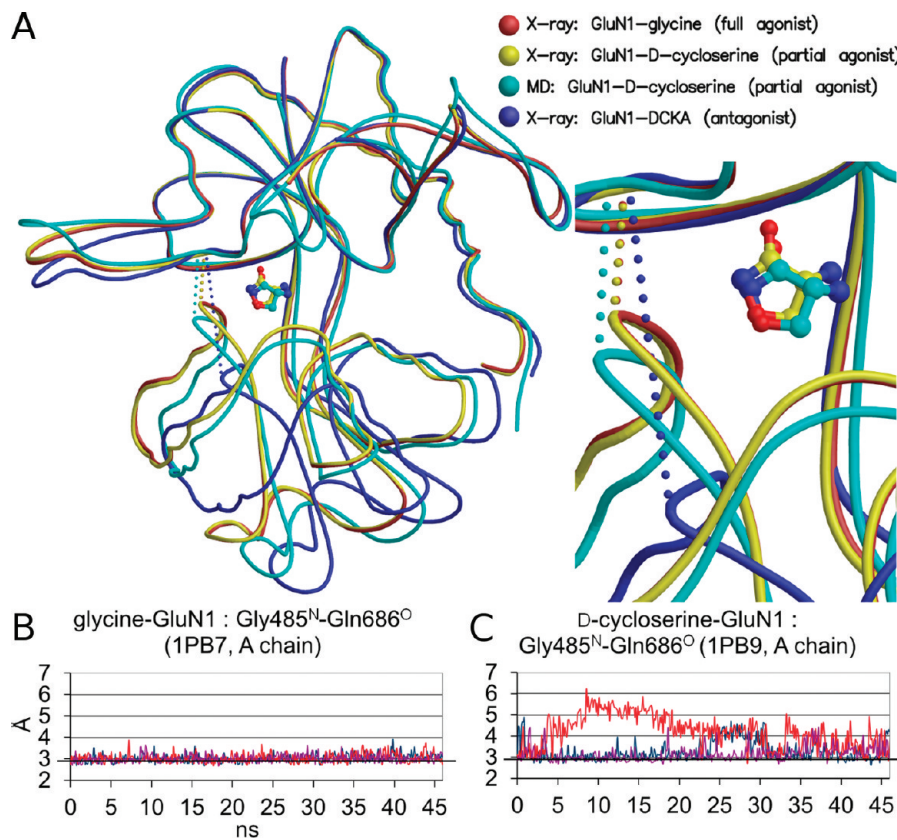


Figure 6. Full agonist and partial agonist simulations with GluN1. (A) The structure comparison shows that both partial agonist D-cycloserine and full agonist glycine bound GluN1-LBC crystal structures (PDB: 1PB9 and 1PB7, respectively) have the same receptor cleft closure stage. However, the antagonist DCKA (PDB: 1PBQ)¹⁰ bound GluN1-LBC differs markedly from the agonist conformations. The close-up indicates that during the MD simulation partial agonist D-cycloserine (cyan) is able to break the IHB (dotted lines; Figure 3C: right panel) and open the GluN1 receptor cleft (snapshot of ~15 ns from no. 2 simulation in panel C; red line). The highly flexible Asn440-Arg448 loop is missing from all crystal structures. The IHB distance is shown for the closed GluN1-LBC MD simulated with (B) full agonist glycine and (C) partial agonist D-cycloserine. See Figure 4 for interpretation.

simulations (Figure 4C–E; Table S2, Supporting Information). Typically, the IHB, which is shown for willardiine and 5-Br-willardiine (Figure 4C and D, respectively), was broken temporarily—for several nanoseconds. Moreover, in the second 5-I-willardiine-GluA2 simulation, the IHB was immediately disrupted, and the cleft stayed open for over half the simulation (as indicated by the red line in Figure 4E; Table S2, Supporting Information). The resulting GluA2 cleft closure and the binding mode of 5-I-willardiine acquired from the simulation closely resemble that seen in the crystal structure (Figure 4A).

The lack of large-scale cleft openings in the closed 5-R-willardiine-GluA2 simulations (Figure 4C–E; Table S2, Supporting Information) was not entirely unexpected, since the partial closure stages of partial agonist-GluA2 crystal structures are not particularly open (Figure 4A; Table S2, Supporting Information). Also, desensitization is known to play a role in 5-R-willardiine-induced partial agonism,¹⁸ and it may affect level of activation. Moreover, we observed temporary full GluA2 cleft closure during our MD simulations with partially open 5-R-willardiine-GluA2 crystal structures (Figure S3, Supporting Information). For example, in all 5-Br-willardiine-GluA2 crystal structure simulations, the IHB atom pair reached H-bonding range for several nanosecond intervals (Figure S3, Supporting Information). This temporary cleft closure is an indication that partial cleft closure is not very stable (or perhaps even necessary)

in partial agonism. It is noteworthy that whenever the IHB was formed during the MD simulations, the H-bonding angles followed closely the ones seen in full agonist-bound crystal structures (Figure S4, Supporting Information).

Full Agonists for GluK2 Cannot Stabilize the Closed Receptor Cleft. At the beginning of the full agonist L-glutamate (Figure 5A and B; Table S3, Supporting Information) and the SYM 2081 (Figure S3 and Table S3, Supporting Information) simulations, the GluK2 cleft stayed stably closed; however, for the remainder of the simulations, the closure was not as tight as it was with GluA2 full agonists (Figure 4B). The IHB was especially discontinuous in the third L-glutamate-GluK2 simulation (magenta line in Figure 5B), which suggests that the GluK2 cleft was closed less tightly than the GluA2 cleft. We also made sure that the starting structure did not affect the stability of the receptor cleft closure by using another closed GluK2 structure (green lines in Figure S3, Supporting Information; PDB: 1S50). The IHB of GluK2 frequently broke and reformed, but again, it was the common denominator for both the crystallized and the MD-simulated full agonist–receptor complexes. The Pro516^O-Glu738^{Ca} distance (Figure 3B) measured from the hinge region of the GluK2 cleft also remained close to the initial crystallization state with both full agonists, as shown by the averages in Table S4, Supporting Information. The aberrant nature of the IHB suggests that the closed GluK2 cleft was not as firmly shut as it

was with GluA2. This means that the GluK2 cleft is able to open during lengthy MD simulations, even with bound full agonists. Therefore, moderately sized partial agonists should be able to keep the GluK2 cleft open, compared to, for example, GluA2. This also explains why there is such a large amount of small GluK2 specific partial agonists (Figure 2).

Bulky Partial Agonists for GluK2 Open the Receptor Cleft. The iGluR-LBCs have been crystallized in complexes with the bulky partial agonists kainate^{6,12} and domoate¹³ (Figure 2) into intermediate closure stages that exist between the open antagonist and the closed full agonist bound conformations (Figures 1 and 5A and Tables S2 and S3, Supporting Information). Our MD simulations indicate that domoate and kainate are able to open the fully closed receptor cleft and produce comparable cleft closure to the original partial agonist bound crystal structures (Figures 5C and S3, Supporting Information, respectively). The whole receptor cleft has to adjust to bind bulky partial agonists, i.e., not only is the IHB affected but also the Pro516^O-Glu738^{Cα} distance (Figure 3B) grows notably (Table S4, Supporting Information). Furthermore, the MD simulations with the partially open GluK2 crystal structures bound by kainate and domoate remained mostly open, though the IHB formed temporarily in the kainate-GluK2 simulations (Figure S3, Supporting Information). This is interesting because it suggests that the GluK2 cleft could close fully with bulky partial agonists such as kainate, and thus, the partially open crystal structure¹² could represent only one possible partial agonist-bound conformation.

Small Partial Agonists Destabilize Closed GluK2 Cleft. A set of small partial agonists for GluK2 (Figure 2)¹⁹ has not been crystallized in complexes with the receptor. To find out how their binding affects the dynamics of GluK2 cleft closure, these small partial agonists were simulated in complexes with closed GluK2-LBC. The closed conformation was chosen because we wanted to see if the MD simulations were able to differentiate full agonists from these small partial agonists, as happened with the bulkier partial agonists. In addition, the Fay et al. docking study suggested that the closed state would be preferable for these partial agonists,¹⁹ and we wanted to find out if the MD simulations would produce different closure stages. The small partial agonists did not necessarily open the cleft, but the IHB of the closed GluK2-LBC (Table S3, Supporting Information) was broken at least temporarily in the simulations. For example, at the beginning of the first L-homocysteine sulfinate-GluK2 simulation, the H-bond broke extensively (blue line in Figure 5D and Table S3, Supporting Information). The H-bond remained broken throughout both the S-sulfo-L-cysteine-GluK2 and L-serine-GluK2 simulations (Figure S3 and Table S3, Supporting Information). Additionally, in two L-aminoacidate-GluK2 simulations, the receptor cleft stayed open for a relatively long time (blue and red lines in Figure 5E and Table S3, Supporting Information), and the cleft closure closely resembled that seen in the crystal structure of the domoate-GluK2 complex (Figure 5A). In contrast to the full agonist L-glutamate, the partial agonist L-aminoacidate has an additional CH₂ on its side chain (Figure 2) that forces the receptor cleft to open, in order to maintain favorable interactions with the D2 lobe (Figure 5A).

IHB distance varied considerably when the small GluK2 partial agonists (Figures 5D and E) were compared to the full agonists (Figure 5B), and yet the GluK2 cleft did not open as effectively as it did with the bulkier partial agonists (Figure 5C). The L-cysteate-GluK2 simulations, with excessive cleft openings, were a notable exception (Table S3, Supporting Information).

Also, the Pro516^O-Glu738^{Cα} distance (Figure 3B) grew with the small partial agonists, especially when maximal distance values were compared to those obtained in the full agonist-GluK2 simulations (Table S4, Supporting Information). Thus, both the bulky (Figure 5C and Table S2, Supporting Information) and small partial agonists (Figure 5D and E and Table S3, Supporting Information) widened the GluK2 cleft in the hinge region, in addition to affecting IHB formation (Figure 3B). From the MD force field standpoint, the small size of these partial agonists (Figure 2) causes fairly low-scale force to be exerted on the closed GluK2 cleft when ligands position themselves inside the ligand-binding pocket. This is the opposite of what occurs when closed iGluR-LBC simulations are performed with antagonists¹⁴ or bulky partial agonists (Figure 5C and Tables S2 and S3, Supporting Information) that open the cleft with ease. We suggest that these small partial agonists are able to open the GluK2-LBC because the GluK2 cleft is not as tightly closed as that of the GluA2 receptor, and therefore, a smaller partial agonist is enough to keep the GluK2 cleft destabilized.

Partial Agonists Disrupt GluN1 Cleft Hydrogen Bonding. A comparison of crystal structures showed that in complexes with GluN1-LBC, full agonists and partial agonists (Figure 3) produce essentially the same closure stages, while antagonists wedge the receptor cleft wide open (Figure 6A). This conformational similarity, seen with full and partial agonists, has led to two hypotheses: (1) Receptor cleft closure is not linked to partial agonism for NMDA receptors, or (2) the cleft can possess different closure stages, and only the closed conformation is crystallized.¹⁰ The MD simulations with the full agonists glycine (Figure 6B and Table S5, Supporting Information) and D-serine (Table S5, Supporting Information) kept the cleft very tightly closed when the IHB (Figure 3C) was inspected (Table S5, Supporting Information). The closed GluN1-LBC crystal structures (Figure 6A and Table S5, Supporting Information) and our MD simulations (Figure 6 and Table S5, Supporting Information) suggest that the GluN1 cleft is more firmly closed than that of the GluA2 or GluK2 subunits.

In MD simulations, the partial agonists ACPC (Table S5, Supporting Information) and the D-cycloserine (Figure 6C and Table S5, Supporting Information) disrupted the IHB and opened the GluN1 cleft. The cleft opening caused by D-cycloserine (Figure 6C) was similar to what was seen with GluA2 and GluK2 bound partial agonists (Figures 4C–E and 5C–E). With D-cycloserine, the IHB broke immediately, and the break was especially extensive in one simulation (red line in Figure 6C and Table S5, Supporting Information). Conversely, in the ACPC-GluN1 simulations, H-bond disruptions were consistent but lesser in scale, and the cleft opening took place only after ~27 ns (data not shown). The tightness of the GluN1 cleft closure (or crystal packing) could be the reason for the delayed opening observed in the partial agonist ACPC–GluN1 complex simulations. Nevertheless, the partial agonist simulations (Figure 6C and Table S5, Supporting Information) indicate that the GluN1 cleft can adjust to a considerably more open conformation with partial agonists than what crystallization has implied thus far. In addition, these results strongly suggest that GluN1 cleft closure stability is linked to partial agonism.

What Disrupts Interdomain Hydrogen Bonding? The atomistic bases for disruptions of the IHB or cleft opening are ligand- and receptor subunit-specific, but there are some common trends. Bulky partial agonists, such as domoate, effectively fill the ligand-binding pocket, linking the D1 and D2 lobes and

preventing full closure of the receptor cleft (Figure 1B). While this process cannot be reproduced in MD simulations if the partial agonist in question is too bulky to be inserted inside the closed ligand-binding pocket, this problem is easily recognizable beforehand. The binding of small partial agonists to the GluK2 cleft causes subtler changes, and the cleft opening can be less pronounced and/or slower. In general, with small GluK2 partial agonists, the α -amino group stays H-bonded to Pro516^O but adjusts itself unfavorably against the hydrophobic side chain of Tyr488. Furthermore, the absence of optimal H-bonding between Thr690 and the γ -carboxylate group of L-glutamate is compensated for with less favorable interactions in the D2 face. These adjustments push the partial agonist toward the residues that line the D2 face, which sometimes results in substantial GluK2 cleft openings (Figure 5A) or, at least, IHB disruptions (Figures 5D and E).

Closer inspection of snapshots from the MD simulations indicates that whenever the IHB is broken, the iGluR-LBC is usually in a conformation similar to that seen in the partial agonist-bound crystal structures. Therefore, the simulated iGluR cleft opening could, in fact, depict actual receptor cleft dynamics with partial agonists (Figures 4–6), as most of the simulated partial agonists (Figure 2) are small enough to allow full closure of the receptor cleft, and the rearrangements that follow the ligand binding (e.g., repulsions) could reopen the cleft. The cleft could then continue to close and open repeatedly, although the ligand stays bound; accordingly, only discontinuous contact between the lobes would occur. The aberrant cleft dynamics, in turn, would also ensure that the IHB atom pair distance, which normally indicates the functional category of a bound ligand (Figure 1), also stays destabilized. Moreover, the labile or intermediate receptor cleft closure would keep the transmembrane ion channel only partially or temporarily open, and weak currents would ensue.

Unfortunately, the effects of the IHB (Figure 3) cannot be studied directly using site-directed mutagenesis as the H-bond is formed between main chain atoms. However, the flexibility seen in partial agonist binding is also supported by previous MD simulation studies by Arinaminpathy et al.^{51,52} The possible link between desensitization and unsteady iGluR cleft closure is worth looking into in the future, as partial agonism and desensitization are known to be related, in some cases.^{15,18}

CONCLUSIONS

The stability of receptor cleft closure varies between subunits in MD simulations. The GluK2 cleft is most likely to open with partial agonists, the GluA2 cleft is less prone to open, and the GluN1 cleft is most resistant to partial agonist-induced opening. For most bulky partial agonists, receptor cleft closure can be recreated routinely using closed iGluR-LBC, since these ligands simply wedge receptor clefts open. The aberrant nature of the IHB (Figures 4C–E) distinguishes 5-R-willardiines as GluA2 specific partial agonists from the simulated full agonists. Similarly, only partial agonists were able to disrupt the IHB in the GluN1 simulations (Figure 6C and Table S5, Supporting Information). In contrast to the inertia of closed GluA2 and GluN1 structures, even relatively small partial agonists (Figure 2) were able to open the GluK2 cleft and disrupt the IHB in MD simulations (Figures 5D and E and Table S3, Supporting Information). The weak link between D1 and D2 lobes in the GluK2 cleft likely explains how relatively small compounds can

act as GluK2 specific partial agonists. This cleft closure instability makes in silico ligand categorization for GluK2 less reliable. Even in the absence of large-scale changes in cleft closure, the IHB was clearly more strained in complexes with GluA2 and GluN1 partial agonists than in complexes with full agonists (Tables S2 and S6, Supporting Information). Thus, the modeling results indicate that, in most cases, partial agonists can be distinguished from full agonists when they are simulated in complexes with closed iGluR-LBCs.

ASSOCIATED CONTENT

S Supporting Information. Four additional figures (Figures S1–S4) and five tables (Tables S1–S5). This material is available free of charge via the Internet at <http://pubs.acs.org>.

AUTHOR INFORMATION

Corresponding Author

*E-mail: olli.t.pentikainen@jyu.fi. Telephone: +358-40-521-6913.

ACKNOWLEDGMENT

This study was funded by the National Doctoral Programme in Informational and Structural Biology (P.A.P.). The Finnish IT Centre for Science (CSC) is acknowledged for their generous computational grants (OTP projects jyy2516 and gc2591).

REFERENCES

- (1) Stern-Bach, Y.; Bettler, B.; Hartley, M.; Sheppard, P. O.; O'Hara, P. J.; Heinemann, S. F. Agonist selectivity of glutamate receptors is specified by two domains structurally related to bacterial amino acid-binding proteins. *Neuron* **1994**, *13*, 1345–1357.
- (2) Safferling, M.; Tichelaar, W.; Kümmel, G.; Jouppila, A.; Kuusinen, A.; Keinänen, K.; Madden, D. R. First images of a glutamate receptor ion channel: oligomeric state and molecular dimensions of GluRB homomers. *Biochemistry* **2001**, *40*, 13948–13953.
- (3) Sobolevsky, A. I.; Rosconi, M. P.; Gouaux, E. X-ray structure, symmetry and mechanism of an AMPA-subtype glutamate receptor. *Nature* **2009**, *462*, 745–756.
- (4) Hollmann, M.; Heinemann, S. Cloned glutamate receptors. *Annu. Rev. Neurosci.* **1994**, *17*, 31–108.
- (5) Johnson, J. W.; Ascher, P. Glycine potentiates the NMDA response in cultured mouse brain neurons. *Nature* **1987**, *325*, 529–531.
- (6) Armstrong, N.; Gouaux, E. Mechanisms for activation and antagonism of an AMPA-sensitive glutamate receptor: crystal structures of the GluR2 ligand binding core. *Neuron* **2000**, *28*, 165–181.
- (7) Hald, H.; Naur, P.; Pickering, D. S.; Sprogøe, D.; Madsen, U.; Timmermann, D. B.; Ahring, P. K.; Lilje fors, T.; Schousboe, A.; Egebjerg, J.; Gajhede, M.; Kastrup, J. S. Partial agonism and antagonism of the ionotropic glutamate receptor iGluRS: structures of the ligand-binding core in complex with domoic acid and 2-amino-3-[5-tert-butyl-3-(phosphonomethoxy)-4-isoxazolyl]propionic acid. *J. Biol. Chem.* **2007**, *282*, 25726–25736.
- (8) Hogner, A.; Greenwood, J. R.; Lilje fors, T.; Lunn, M.; Egebjerg, J.; Larsen, I. K.; Gouaux, E.; Kastrup, J. S. Competitive antagonism of AMPA receptors by ligands of different classes: crystal structure of ATPO bound to the GluR2 ligand-binding core, in comparison with DNQX. *J. Med. Chem.* **2003**, *46*, 214–221.
- (9) Mayer, M. L.; Ghosal, A.; Dolman, N. P.; Jane, D. E. Crystal structures of the kainate receptor GluR5 ligand binding core dimer with novel GluR5-selective antagonists. *J. Neurosci.* **2006**, *26*, 2852–2861.
- (10) Furukawa, H.; Gouaux, E. Mechanisms of activation, inhibition and specificity: crystal structures of the NMDA receptor NR1 ligand-binding core. *EMBO J.* **2003**, *22*, 2873–2885.

- (11) Jin, R.; Banke, T. G.; Mayer, M. L.; Traynelis, S. F.; Gouaux, E. Structural basis for partial agonist action at ionotropic glutamate receptors. *Nat. Neurosci.* **2003**, *6*, 803–810.
- (12) Mayer, M. L. Crystal structures of the GluR5 and GluR6 ligand binding cores: molecular mechanisms underlying kainate receptor selectivity. *Neuron* **2005**, *45*, 539–552.
- (13) Nanao, M. H.; Green, T.; Stern-Bach, Y.; Heinemann, S. F.; Choe, S. Structure of the kainate receptor subunit GluR6 agonist-binding domain complexed with domoic acid. *Proc. Natl. Acad. Sci. U.S.A.* **2005**, *102*, 1708–1713.
- (14) Postila, P. A.; Swanson, G. T.; Pentikäinen, O. T. Exploring kainate receptor pharmacology using molecular dynamics simulations. *Neuropharmacology* **2010**, *58*, 515–527.
- (15) Lash, L. L.; Sanders, J. M.; Akiyama, N.; Shoji, M.; Postila, P.; Pentikäinen, O. T.; Sasaki, M.; Sakai, R.; Swanson, G. T. Novel analogs and stereoisomers of the marine toxin neodysiherbaine with specificity for kainate receptors. *J. Pharmacol. Exp. Ther.* **2008**, *324*, 484–496.
- (16) Sanders, J. M.; Pentikäinen, O. T.; Settimio, L.; Pentikäinen, U.; Shoji, M.; Sasaki, M.; Sakai, R.; Johnson, M. S.; Swanson, G. T. Determination of binding site residues responsible for the subunit selectivity of novel marine-derived compounds on kainate receptors. *Mol. Pharmacol.* **2006**, *69*, 1849–1860.
- (17) Frydenvang, K.; Lash, L. L.; Naur, P.; Postila, P. A.; Pickering, D. S.; Smith, C. M.; Gajhede, M.; Sasaki, M.; Sakai, R.; Pentikäinen, O. T.; Swanson, G. T.; Kastrup, J. S. Full domain closure of the ligand-binding core of the ionotropic glutamate receptor iGluR5 induced by the high affinity agonist dysiherbaine and the functional antagonist 8,9-dideoxyneodysiherbaine. *J. Biol. Chem.* **2009**, *284*, 14219–14229.
- (18) Patneau, D. K.; Mayer, M. L.; Jane, D. E.; Watkins, J. C. Activation and desensitization of AMPA/kainate receptors by novel derivatives of willardiine. *J. Neurosci.* **1992**, *12*, 595–606.
- (19) Fay, A. L.; Corbeil, C. R.; Brown, P.; Moitessier, N.; Bowie, D. Functional characterization and in silico docking of full and partial GluK2 kainate receptor agonists. *Mol. Pharmacol.* **2009**, *75*, 1096–1107.
- (20) Sun, Y.; Olson, R.; Horning, M.; Armstrong, N.; Mayer, M.; Gouaux, E. Mechanism of glutamate receptor desensitization. *Nature* **2002**, *417*, 245–253.
- (21) Plessted, A. J. R.; Mayer, M. L. Structure and mechanism of kainate receptor modulation by anions. *Neuron* **2007**, *53*, 829–841.
- (22) Menuz, K.; Stroud, R. M.; Nicoll, R. A.; Hays, F. A. TARP auxiliary subunits switch AMPA receptor antagonists into partial agonists. *Science* **2007**, *318*, 815–817.
- (23) Berman, H. M.; Westbrook, J.; Feng, Z.; Gilliland, G.; Bhat, T. N.; Weissig, H.; Shindyalov, I. N.; Bourne, P. E. The Protein Data Bank. *Nucleic Acids Res.* **2000**, *28*, 235–242.
- (24) Keinänen, K.; Wisden, W.; Sommer, B.; Werner, P.; Herb, A.; Verdoorn, T. A.; Sakmann, B.; Seeburg, P. H. A family of AMPA-selective glutamate receptors. *Science* **1990**, *249*, 556–560.
- (25) Lehtonen, J. V.; Still, D.; Rantanen, V.; Ekholm, J.; Björklund, D.; Iftikhar, Z.; Huhtala, M.; Repo, S.; Jussila, A.; Jaakkola, J.; Pentikäinen, O.; Nyrönen, T.; Salminen, T.; Gyllenberg, M.; Johnson, M. S. BODIL: a molecular modeling environment for structure-function analysis and drug design. *J. Comput.-Aided Mol. Des.* **2004**, *18*, 401–419.
- (26) Sali, A.; Blundell, T. L. Comparative protein modelling by satisfaction of spatial restraints. *J. Mol. Biol.* **1993**, *234*, 779–815.
- (27) Inanobe, A.; Furukawa, H.; Gouaux, E. Mechanism of partial agonist action at the NR1 subunit of NMDA receptors. *Neuron* **2005**, *47*, 71–84.
- (28) Moriyoshi, K.; Masu, M.; Ishii, T.; Shigemoto, R.; Mizuno, N.; Nakanishi, S. Molecular cloning and characterization of the rat NMDA receptor. *Nature* **1991**, *354*, 31–37.
- (29) Petrey, D.; Xiang, Z.; Tang, C. L.; Xie, L.; Gimpelev, M.; Mitros, T.; Soto, C. S.; Goldsmith-Fischman, S.; Kernytsky, A.; Schlessinger, A.; Koh, I. Y. Y.; Alexov, E.; Honig, B. Using multiple structure alignments, fast model building, and energetic analysis in fold recognition and homology modeling. *Proteins* **2003**, *53* (Suppl. 6), 430–435.
- (30) Bayly, C.; Cieplak, P.; Cornell, W.; Kollman, P. A well-behaved electrostatic potential based method using charge restraints for deriving atomic charges: the RESP model. *J. Phys. Chem.* **1993**, *97*, 10269–10280.
- (31) Cieplak, P.; Cornell, W.; Bayly, C.; Kollman, P. Application of the multimolecule and multiconformational RESP methodology to biopolymers-charge derivation for DNA, RNA, and proteins. *J. Comput. Chem.* **1995**, *16*, 1357–1377.
- (32) Cornell, W.; Cieplak, P.; Bayly, C.; Kollman, P. Application of the RESP Charges to Calculate Conformational Energies, Hydrogen Bond Energies, and Free Energies of Solvation. *J. Am. Chem. Soc.* **1993**, *115*, 9620–9631.
- (33) Singh, U. C.; Kollman, P. A. An approach to computing electrostatic charges for molecules. *J. Comput. Chem.* **1984**, *5*, 129–145.
- (34) Jones, G.; Willett, P.; Glen, R. C. Molecular recognition of receptor sites using a genetic algorithm with a description of desolvation. *J. Mol. Biol.* **1995**, *245*, 43–53.
- (35) Jones, G.; Willett, P.; Glen, R. C.; Leach, A. R.; Taylor, R. Development and validation of a genetic algorithm for flexible docking. *J. Mol. Biol.* **1997**, *267*, 727–748.
- (36) Wang, H.; Liu, Y.; Huai, Q.; Cai, J.; Zoragh, R.; Francis, S. H.; Corbin, J. D.; Robinson, H.; Xin, Z.; Lin, G.; Ke, H. Multiple conformations of phosphodiesterase-5: implications for enzyme function and drug development. *J. Biol. Chem.* **2006**, *281*, 21469–21479.
- (37) Phillips, J. C.; Braun, R.; Wang, W.; Gumbart, J.; Tajkhorshid, E.; Villa, E.; Chipot, C.; Skeel, R. D.; Kalé, L.; Schulten, K. Scalable molecular dynamics with NAMD. *J. Comput. Chem.* **2005**, *26*, 1781–1802.
- (38) Feller, S.; Zhang, Y.; Pastor, R.; Brooks, B. Constant pressure molecular dynamics simulation: the Langevin piston method. *J. Chem. Phys.* **1995**, *103*, 4613–4621.
- (39) Schlick, T.; Skeel, R. D.; Brunger, A. T.; Kalé, L. V.; Board, J. A. J.; Hermans, J.; Schulten, K. Algorithmic Challenges in Computational Molecular Biophysics. *J. Comput. Phys.* **1999**, *151*, 9–48.
- (40) Darden, T.; York, J.; Pedersen, L. Particle mesh Ewald: An $\mathcal{O}(N \log N)$ method for Ewald sums in large systems. *J. Chem. Phys.* **1993**, *98*, 10089–10092.
- (41) Essmann, U.; Perera, L.; Berkowitz, M. L. The Origin of the Hydration Interaction of Lipid Bilayers from MD Simulation of Dipalmitoylphosphatidylcholine Membranes in Gel and Liquid Crystalline Phases. *J. Chem. Phys.* **1995**, *103*, 8577–8593.
- (42) Sagui, C.; Darden, T. A. Molecular dynamics simulations of biomolecules: long-range electrostatic effects. *Annu. Rev. Biophys. Biomol. Struct.* **1999**, *28*, 155–179.
- (43) Toukmaji, A.; Sagui, C.; Board, J.; Darden, T. Efficient particle-mesh Ewald based approach to fixed and induced dipolar interactions. *J. Chem. Phys.* **2000**, *113*, 10913–10927.
- (44) Ryckaert, J.; Ciccotti, G.; Berendsen, H. Numerical integration of the Cartesian equations of proteins and nucleic acids. *J. Comput. Phys.* **1977**, *23*, 327–341.
- (45) Kraulis, P. MOLSCRIPT: A Program to Produce Both Detailed and Schematic Plots of Protein Structures. *J. Appl. Crystallogr.* **1991**, *24*, 946–950.
- (46) Merritt, E. A.; Bacon, D. J. Raster3D: photorealistic molecular graphics. *Methods Enzymol.* **1997**, *277*, 505–524.
- (47) Gill, M. B.; Vivithanaporn, P.; Swanson, G. T. Glutamate binding and conformational flexibility of ligand-binding domains are critical early determinants of efficient kainate receptor biogenesis. *J. Biol. Chem.* **2009**, *284*, 14503–14512.
- (48) Lau, A. Y.; Roux, B. The free energy landscapes governing conformational changes in a glutamate receptor ligand-binding domain. *Structure* **2007**, *15*, 1203–1214.
- (49) Penn, A. C.; Williams, S. R.; Greger, I. H. Gating motions underlie AMPA receptor secretion from the endoplasmic reticulum. *EMBO J.* **2008**, *27*, 3056–3068.
- (50) Robert, A.; Armstrong, N.; Gouaux, J. E.; Howe, J. R. AMPA receptor binding cleft mutations that alter affinity, efficacy, and recovery from desensitization. *J. Neurosci.* **2005**, *25*, 3752–3762.

- (S1) Arinaminpathy, Y.; Sansom, M. S. P.; Biggin, P. C. Binding site flexibility: molecular simulation of partial and full agonists within a glutamate receptor. *Mol. Pharmacol.* **2006**, *69*, 11–18.
- (S2) Arinaminpathy, Y.; Sansom, M. S. P.; Biggin, P. C. Molecular dynamics simulations of the ligand-binding domain of the ionotropic glutamate receptor GluR2. *Biophys. J.* **2002**, *82*, 676–683.